Decoupling Copolymer, Lipid and Carbon Nanotube Interactions in Hybrid, Biomimetic Vesicles

Joshua A Hammons,[a] Helgi I. Ingólfsson [b], Jeremy Sanborn [c], Jonathan R.I. Lee [a], Tim Carpenter [b], Ramya Tunuguntla [c], Yun-Chiao Yao [c], Thomas M. Weiss, Aleksandr Noy [c,e] and Tony Van Buuren[a]

S.1. SAXS Model Fitting

The SAXS data collected from the different vesicle bilayers was modeled using three separate approaches to extract the bilayer morphology. The Guinier approximation only applies to the relatively low-q portion of the scattering from a given phase where the intensity decreases in a "knee-like" fashion.[1] Therefore, only the portion of the I(q) curve where the intensity decreased in a "knee-like" fashion was fit to the Guinier approximation[1] by the equation:

(S1).

$$I(q) = G \exp\left(\frac{-q^2 R_g^2}{3}\right)$$

where G is a scaling factor that is proportional to the contrast, number density and volume and Rg is the radius of gyration. Equation 1 is a rather robust approximation in small angle scattering, as it only assumes a center of symmetry.[1] Because the vesicle radii are much larger than the bilayers, the local shape of the bilayer is approximated as a low aspect ratio disc that has the relationship $t_{SAXS} = R_g\sqrt{12}$.[1] The model fits of Equation 1 to all of the data are shown in Figure S 1 for the hybrid vesicles without CNTP and Figure S 2 with CNTP.

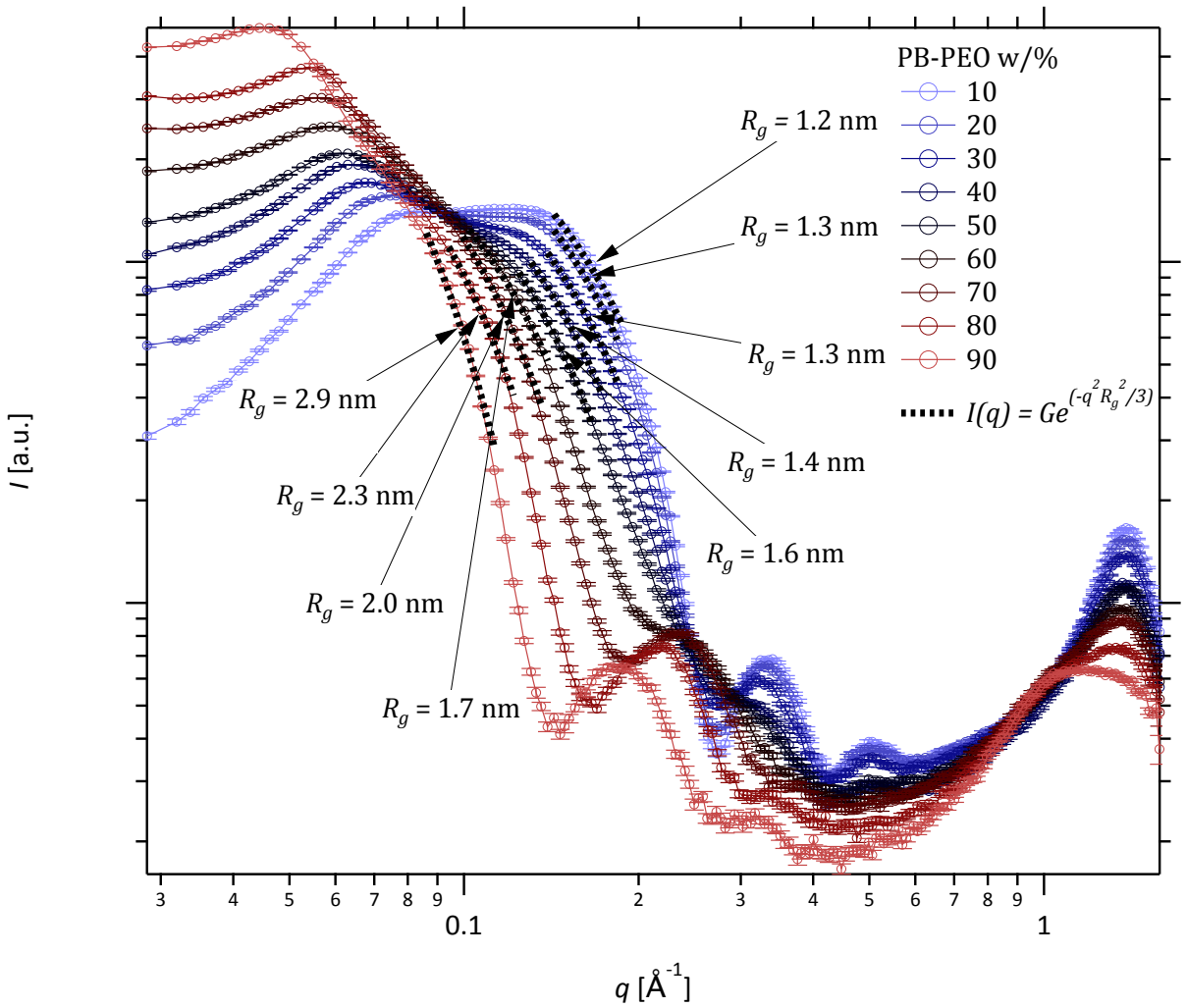

Figure S 1 log-log plot of SAXS data obtained from the hybrid copolymer-lipid vesicles (open circles) with the model fitting obtained from the Guinier approximation (dashed lines) for each weight percentage of copolymer.

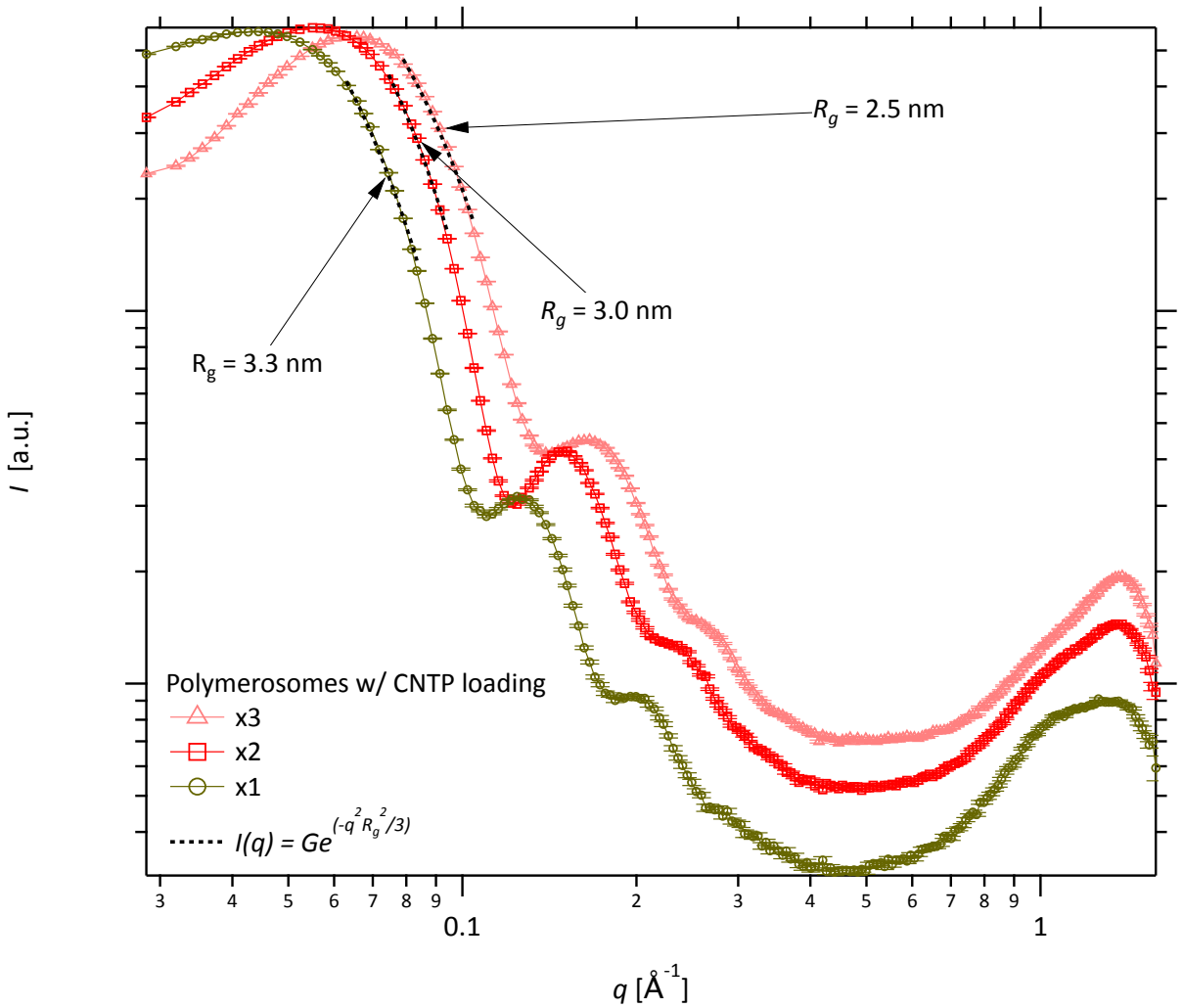

Figure S 2 log-log plot of SAXS data obtained from the hybrid copolymer-lipid vesicles with x1 CNTP loading (open circles), x2 CNTP loading (open squares), and x3 CNTP loading (open triangles) with the model fitting obtained from the Guinier approximation (dashed lines).

Simple Bilayer Modeling

While Equation 1 is a simple, robust approximation, it contains some bias and does not contain any information about the internal heterogeneity of the bilayer. Equation S 1 only applies to the low-q limit of the scattered intensity, and therefore only a small portion of the I(q) curve was fit, which introduces some bias. Furthermore, the broad peak at low-q (Figure S 1) indicates some interference scattering that will also skew the results because the Guinier approximation assumes the phase is dilute.[1] The simple (symmetric) bilayer function contains only four fit parameters: the maximum scattering length density of the outer hydrophilic regions, ρ_o, and inner hydrophobic region, ρ_i, and the corresponding thickness of the inner, t_i, and outer region, t_o, which are used as inputs to a normalized Gaussian functions,Γ, that have maximum values of 1:

(S2).

$$\rho_v(r,\rho_i,\rho_o,t_i,t_o)$$
$$= \left[\rho_o - \rho_{H_2O}\right]\Gamma\left(\frac{t_o}{2.3548}, R_v + \frac{t_o}{2}, r\right)$$
$$+ \left[\rho_i - \rho_{H_2O}\right]\Gamma\left(\frac{t_i}{2.3548}, R_v + t_o + \frac{t_i}{2}, r\right)$$
$$+ \left[\rho_o - \rho_{H_2O}\right]\Gamma\left(\frac{t_o}{2.3548}, R_v + \frac{t_o}{2} + t_i + t_o, r\right) + \rho_{H_2O}$$

where R_v is the inner radius of the vesicle, ρ_{H_2O} is the scattering length density of water (9.42 x 10^{10} cm^{-2}) and the factor 2.3548 converts the thickness to a standard deviation; within the fitting routine, either ρ_o or ρ_i is fit, since it is only δ_{io} that is unique. Converting the simple function in Equation S2 to a scattered intensity, $I_v(q)$ is accomplished by assuming that the vesicles are spherical (Equation 4 in the main text). Equation S 2 assumes that the bilayer is symmetric, which is sufficient to model the SAXS data collected with low copolymer loadings and SAXS data collected from hybrid vesicles with CNTP. Additional parameters can be incorporated into Equation S 2 that accommodate varying amounts of asymmetry[2]. An attempt was made to treat the outer, hydrophilic, regions separately (two additional parameters) to fit the copolymer-lipid hybrid vesicle bilayers. However, there was no significant improvement on the fit quality. In cases where Equation S 2 resulted in significant misfit, simulated annealing was used to refine the bilayer structure.

In addition to the bilayer scattering, the high-q scattering that was attributed to the kinetic order from the DOPC and $PB_{22}PEO_{14}$ in the main article was modelled with two additional Gaussian functions and a flat background, *b*. In total, there were 5 fit parameters that were fit to the bilayer scattering and 5 fit parameters fit to the high-q scattering; we note that the refinement of the high-q fit parameters was able to account for the transition from low-q to high-q scattering but was not able to achieve a fit that was as good as that obtained with the multi-peak package with Igor pro.

Simulated Annealing

The electron density profile from the hybrid lipid-copolymer vesicle membranes could not be modelled well using Equation S2 for the bilayer membrane. In order to understand how the membranes differ from an otherwise simple bilayer, simulated annealing was employed. The purpose of this approach is to randomly perturb an otherwise simple function obtained by least squares fitting of Equation 1 and Equation S2 and compare the perturbations with the profiles of the dioleoyl and PB groups obtained by MD. In this way, the results are combined together to understand the bilayer morphology. The general procedure is outlined in detail below.

In order to randomize the candidate functions a random number generator was used to create 400 randomly spaced points between R_v and $R_v+2t_o+t_i$, using the numpy package for python. Next, the data were fit to Equation 1 and Equation S2 to obtain a simple function of $\rho_v(r)$ that closely resembles the actual bilayer morphology. At this point, the simulated annealing begins by perturbing $\rho_v(r)$ using a random gaussian function that has a mean location between 0 and 400,

a standard deviation between 1 and 10 points and a maximum amplitude between -0.1 x 10^{10} cm^{-2} and 0.1 x 10^{10} cm^{-2}. This gaussian function is added to the function $\rho_v(r)$ and the χ^2 is calculated by the equation

(S3).

$$\chi^2 = \left[\frac{I(q) - I_v(q)}{e(q)}\right]^2$$

where $I(q)$ is the background subtracted data and $e(q)$ is the error obtained from the integration performed by the Nika package[3] for Igor Pro. Each move is evaluated and accepted depending on the temperature and the change in χ^2 compared with the previous value; the temperature is a non-physical parameter and is therefore unitless. This routine is summarized by the following steps:

1) Establish the total number of steps, N, a maximum temperature, T_{max}, and a minimum temperature, T_{min}.
2) Calculate the initial χ^2 of the system.
3) Perturb the function $\rho_v(r)$ with a randomly chosen Gaussian function.
4) Calculate the new χ^2 and temperature, T, of the system by the equation:

(S4).

$$T = T_{max} e^{-\frac{i}{N} \log^{T_{max}}/_{T_{min}}}$$

5) The new state obtained in step 4 is accepted if it meets one of the following conditions:

(S5).

$$[\chi_i^2 - \chi_{i-1}^2] < 0$$

(S6).

$$e^{-\frac{[\chi_i^2 - \chi_{i-1}^2]}{T}} > U([0,1])$$

where $U([0,1])$ denotes a random floating-point number between 0 and 1.

6) Steps 3 – 5 are repeated for N steps.

The optimal T_{max} was determined to be 500 and T_{min} was 0.1 for these data. The number of steps, N, was varied between 20000 and 30000. The simulated annealing procedure was repeated more than 30 times for each composition, each time generated a new random set of points for $\rho_v(r)$. The candidate functions with the lowest value of are shown in Figure S3 for all of the hybrid compositions. All of the candidate functions from each simulated annealing procedure can be found in Figures S 4 through S13 with the initial bilayer function.

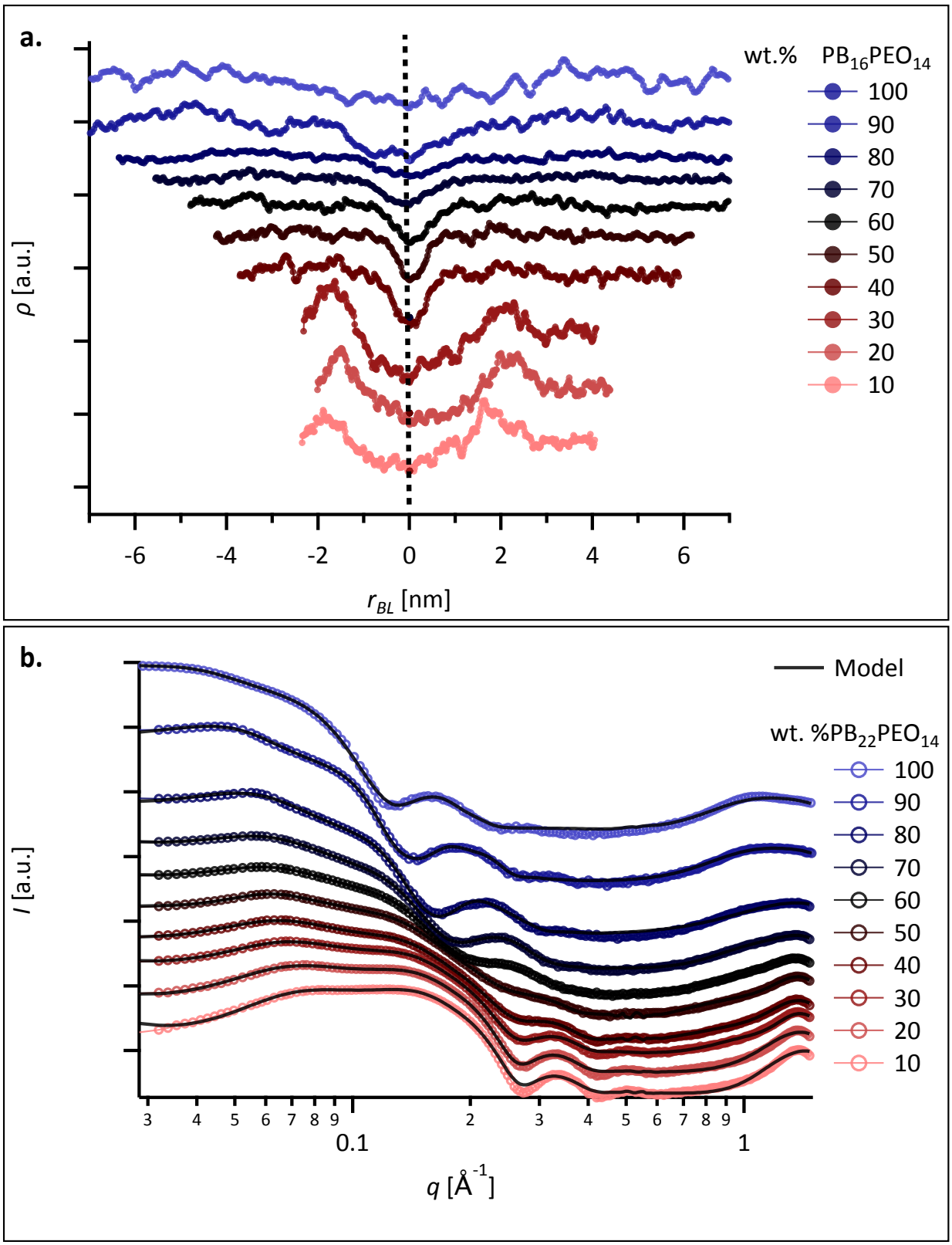

Figure S 3 log-log plot of SAXS data and modelling (a) the resulting the ρ(r) profiles obtained by simulated annealing of the SAXS data, and (c) the model fits to the data.

All Annealing Results

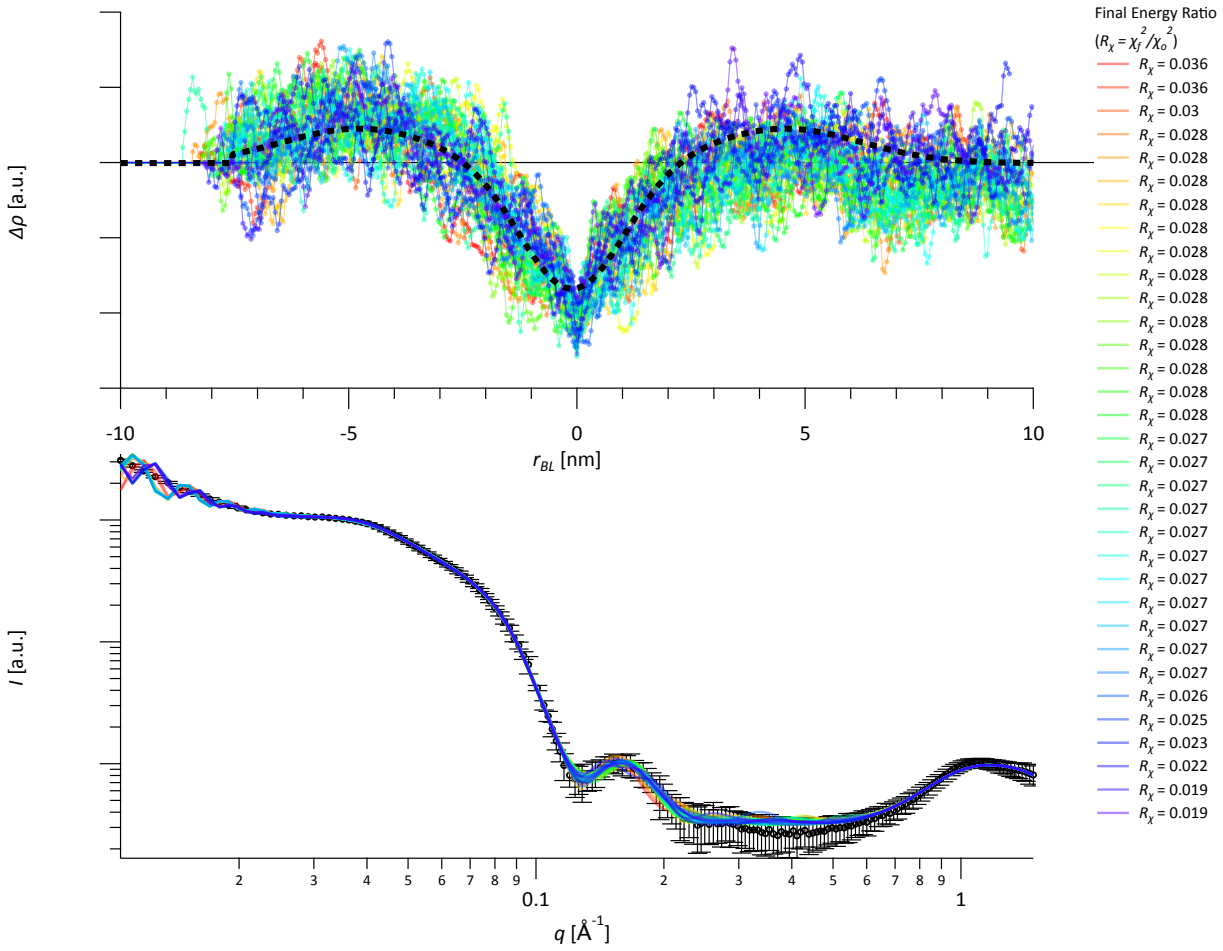

Figure S 4 (bottom) a log-log plot of the SAXS data collected from 100% PB-PEO polymerosomes (black) with the model fits obtained from simulated annealing (colored) and (top) the resulting radial contrast functions through the bilayer, Δρ, (colored) compared with the initial radial contrast function (dashed line) and the zero (solvent) line (black line).

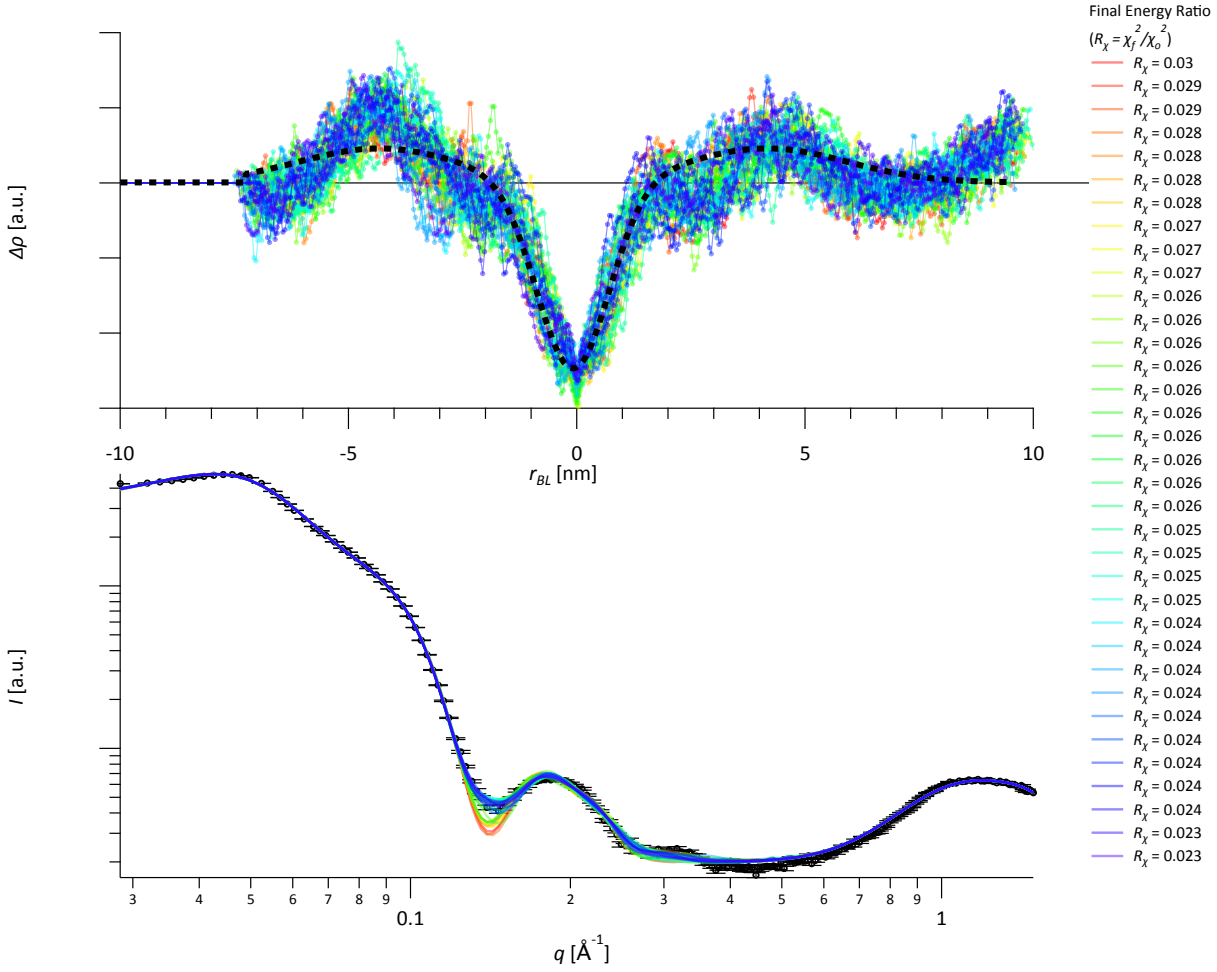

Figure S 5 (bottom) a log-log plot of the SAXS data collected from 90 % PB-PEO hybrid vesicles (black) with the model fits obtained from simulated annealing (colored) and (top) the resulting radial contrast functions through the bilayer, Δρ, (colored) compared with the initial radial contrast function (dashed line) and the zero (solvent) line (black line).

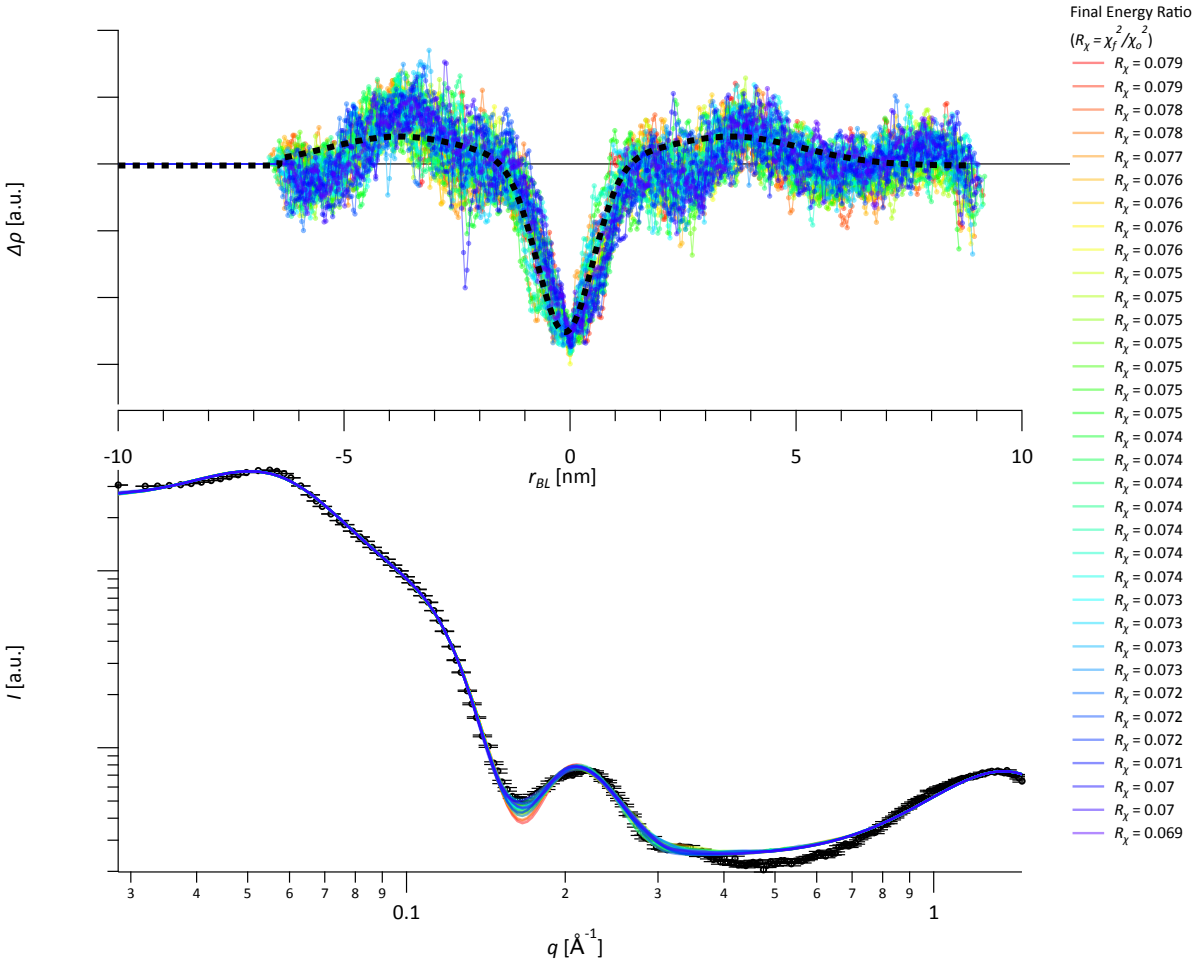

Figure S 6 (bottom) a log-log plot of the SAXS data collected from 80 % PB-PEO hybrid vesicles (black) with the model fits obtained from simulated annealing (colored) and (top) the resulting radial contrast functions through the bilayer, Δρ, (colored) compared with the initial radial contrast function (dashed line) and the zero (solvent) line (black line).

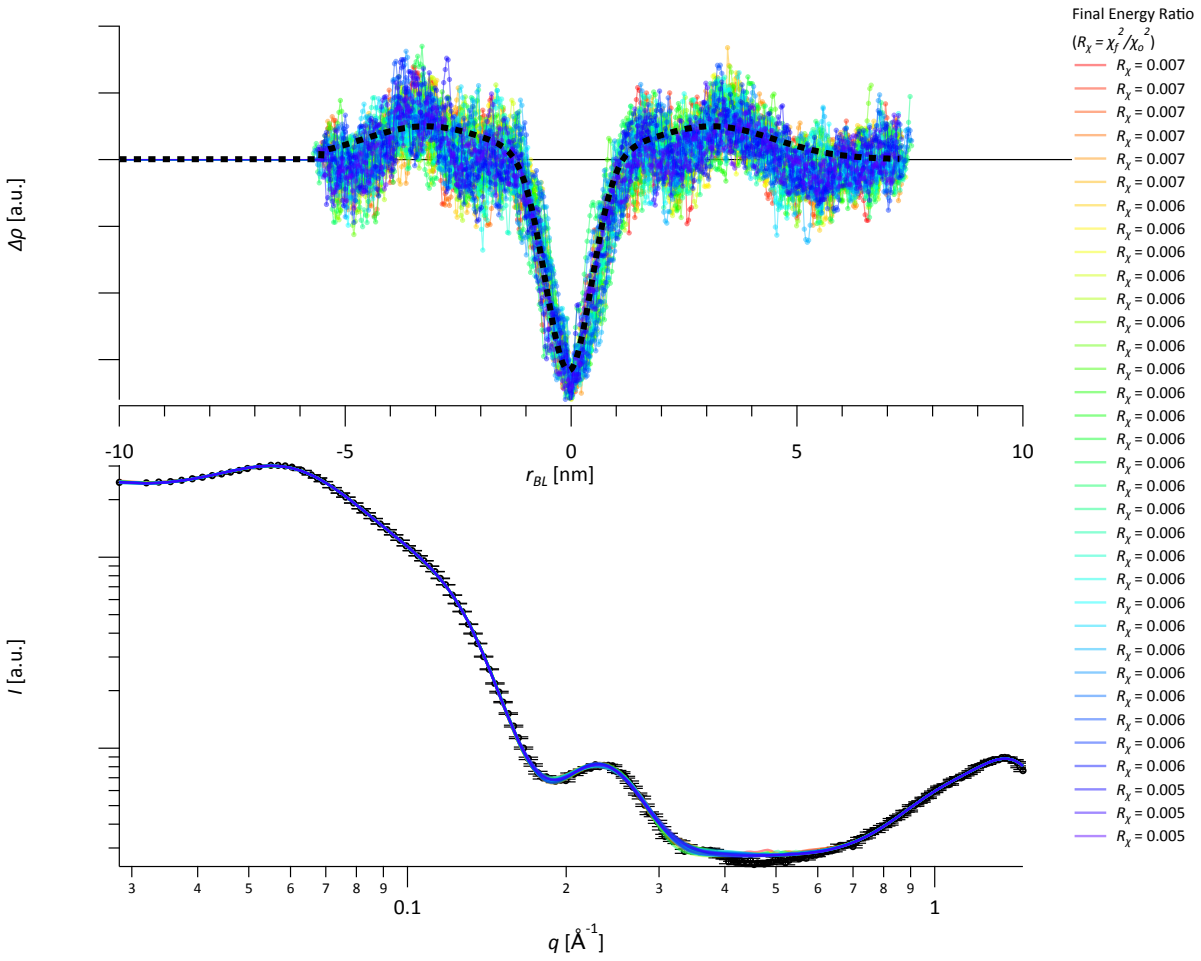

Figure S 7 (bottom) a log-log plot of the SAXS data collected from 70 % PB-PEO hybrid vesicles (black) with the model fits obtained from simulated annealing (colored) and (top) the resulting radial contrast functions through the bilayer, Δρ, (colored) compared with the initial radial contrast function (dashed line) and the zero (solvent) line (black line).

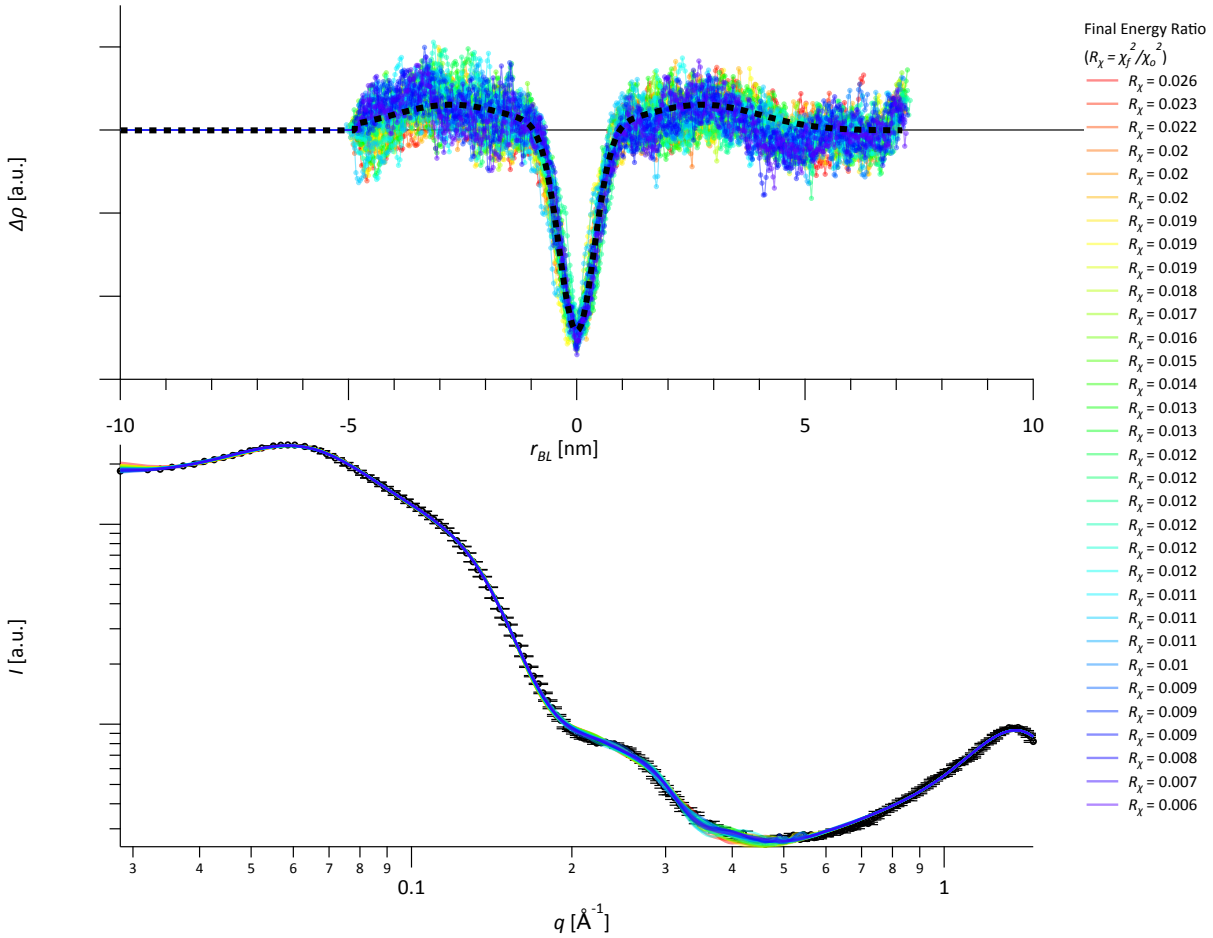

Figure S 8 (bottom) a log-log plot of the SAXS data collected from 60 % PB-PEO hybrid vesicles (black) with the model fits obtained from simulated annealing (colored) and (top) the resulting radial contrast functions through the bilayer, Δρ, (colored) compared with the initial radial contrast function (dashed line) and the zero (solvent) line (black line).

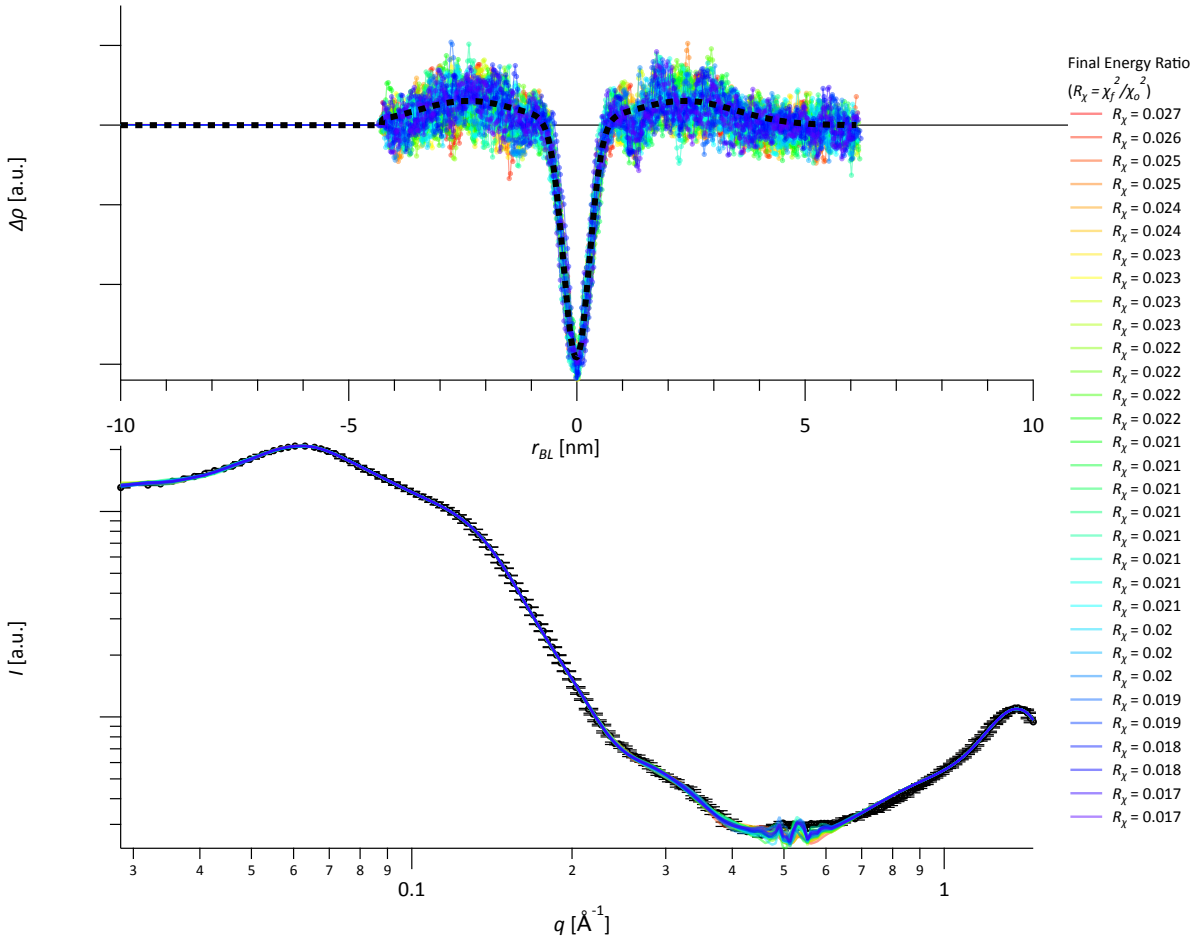

Figure S 9 (bottom) a log-log plot of the SAXS data collected from 50 % PB-PEO hybrid vesicles (black) with the model fits obtained from simulated annealing (colored) and (top) the resulting radial contrast functions through the bilayer, Δρ, (colored) compared with the initial radial contrast function (dashed line) and the zero (solvent) line (black line).

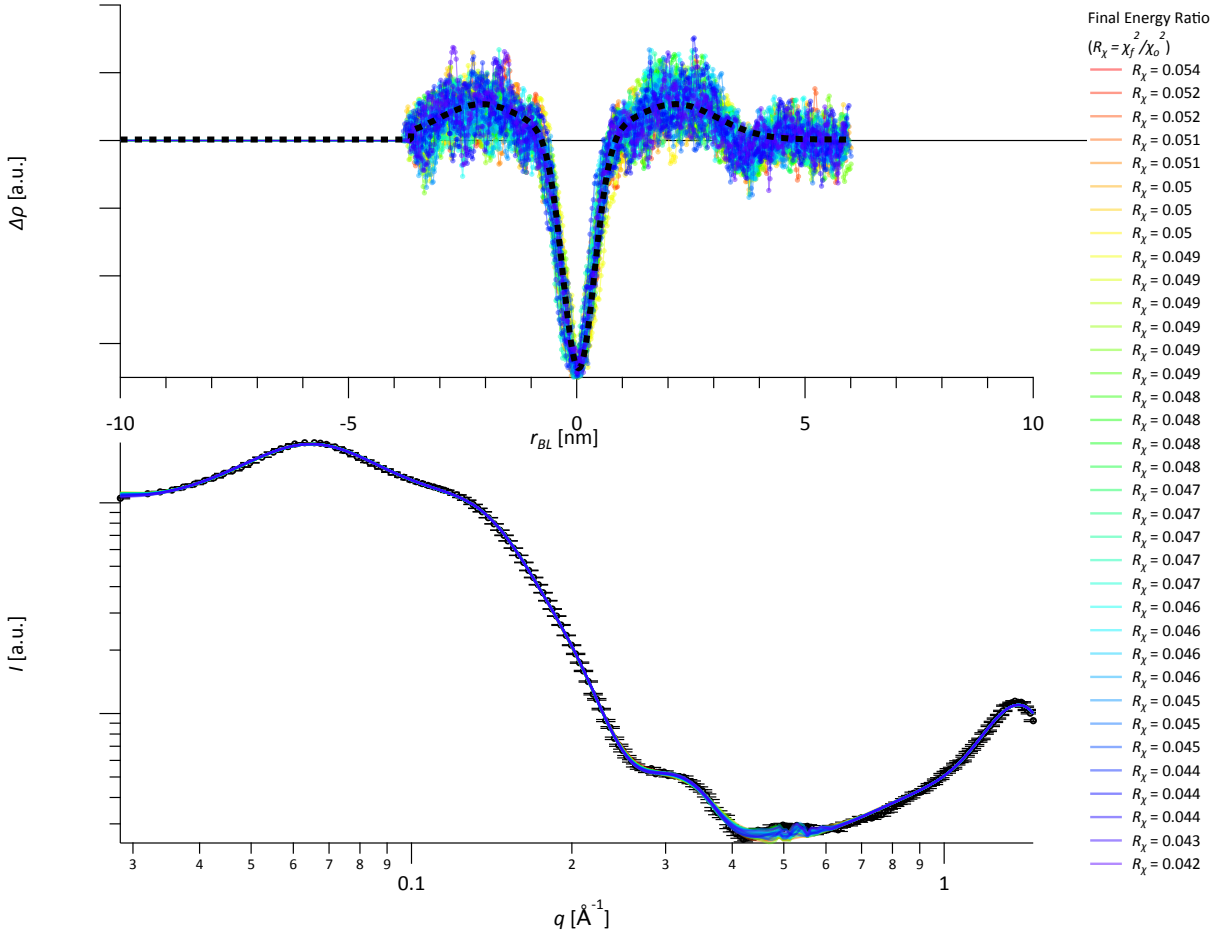

Figure S 10 (bottom) a log-log plot of the SAXS data collected from 40 % PB-PEO hybrid vesicles (black) with the model fits obtained from simulated annealing (colored) and (top) the resulting radial contrast functions through the bilayer, Δρ, (colored) compared with the initial radial contrast function (dashed line) and the zero (solvent) line (black line).

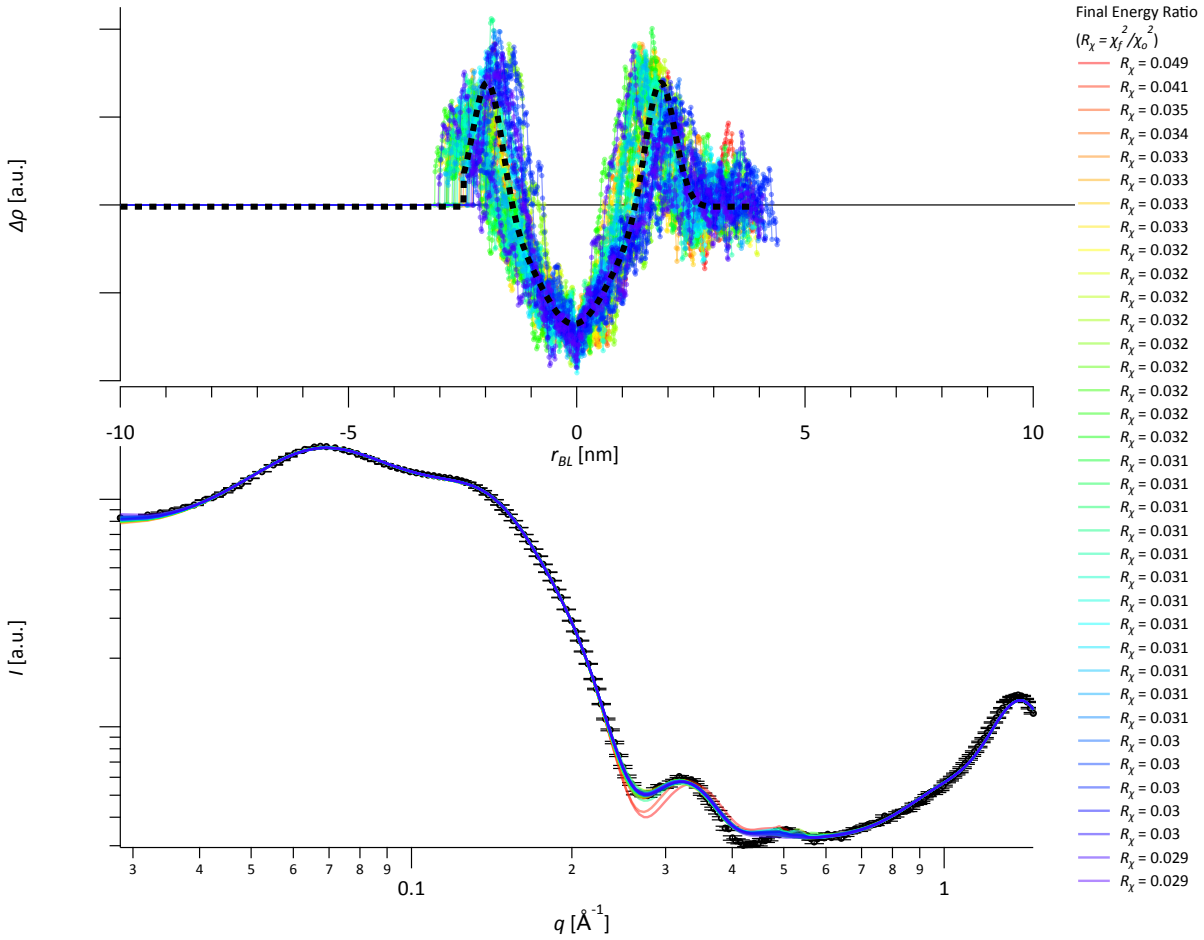

Figure S 11 (bottom) a log-log plot of the SAXS data collected from 30 % PB-PEO hybrid vesicles (black) with the model fits obtained from simulated annealing (colored) and (top) the resulting radial contrast functions through the bilayer, Δρ, (colored) compared with the initial radial contrast function (dashed line) and the zero (solvent) line (black line).

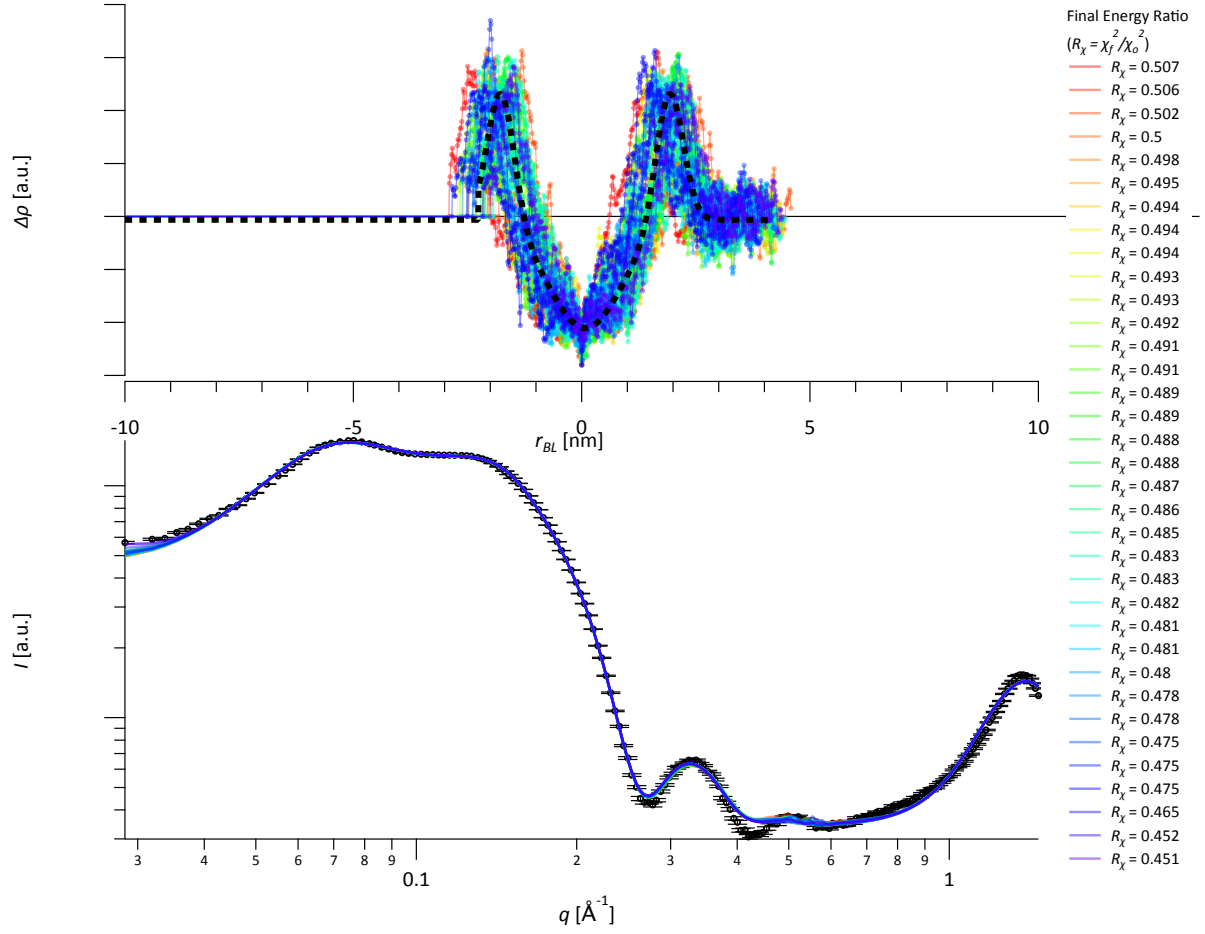

Figure S 12 (bottom) a log-log plot of the SAXS data collected from 20 % PB-PEO hybrid vesicles (black) with the model fits obtained from simulated annealing (colored) and (top) the resulting radial contrast functions through the bilayer, Δρ, (colored) compared with the initial radial contrast function (dashed line) and the zero (solvent) line (black line).

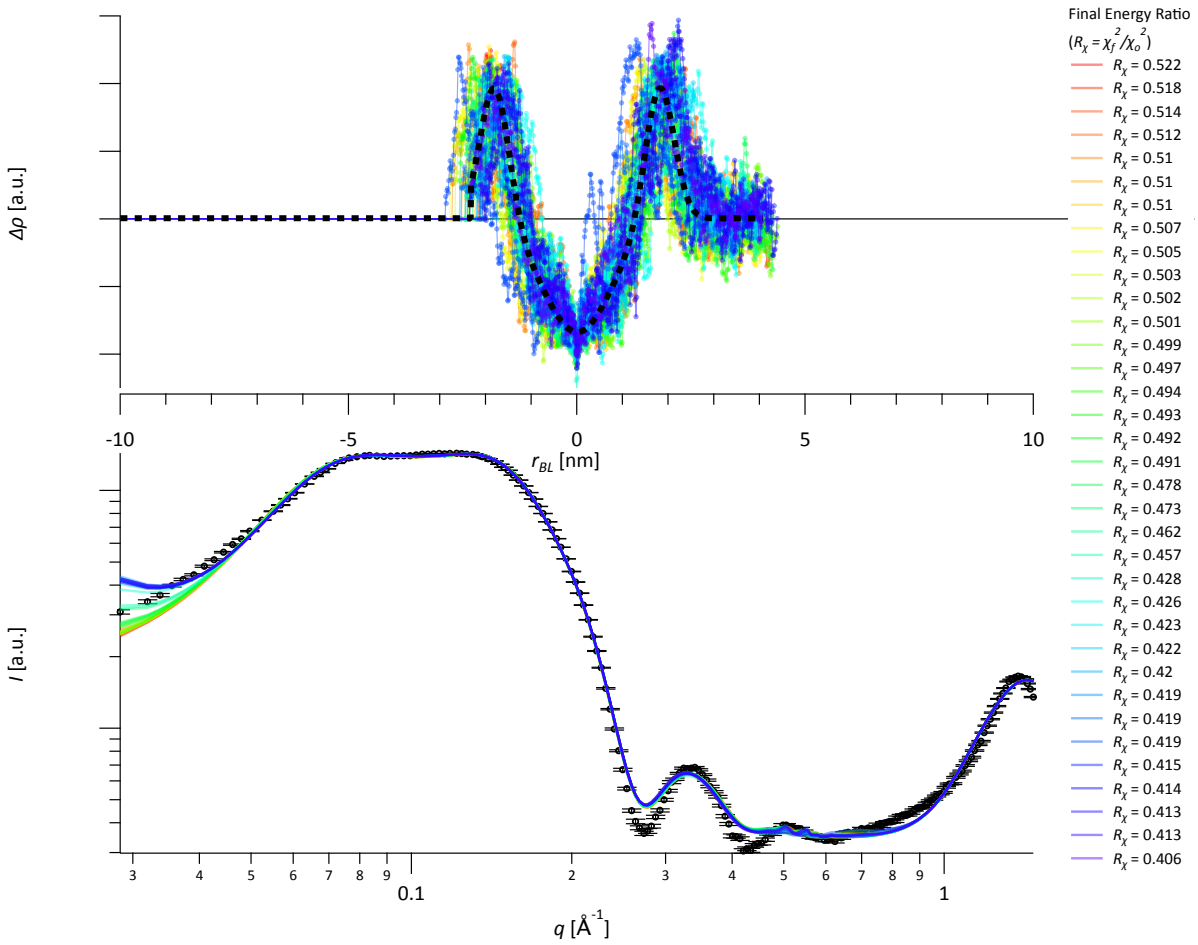

Figure S 13 (bottom) a log-log plot of the SAXS data collected from 10 % PB-PEO hybrid vesicles (black) with the model fits obtained from simulated annealing (colored) and (top) the resulting radial contrast functions through the bilayer, Δρ, (colored) compared with the initial radial contrast function (dashed line) and the zero (solvent) line (black line).

S.2 Molecular Dynamics Simulations

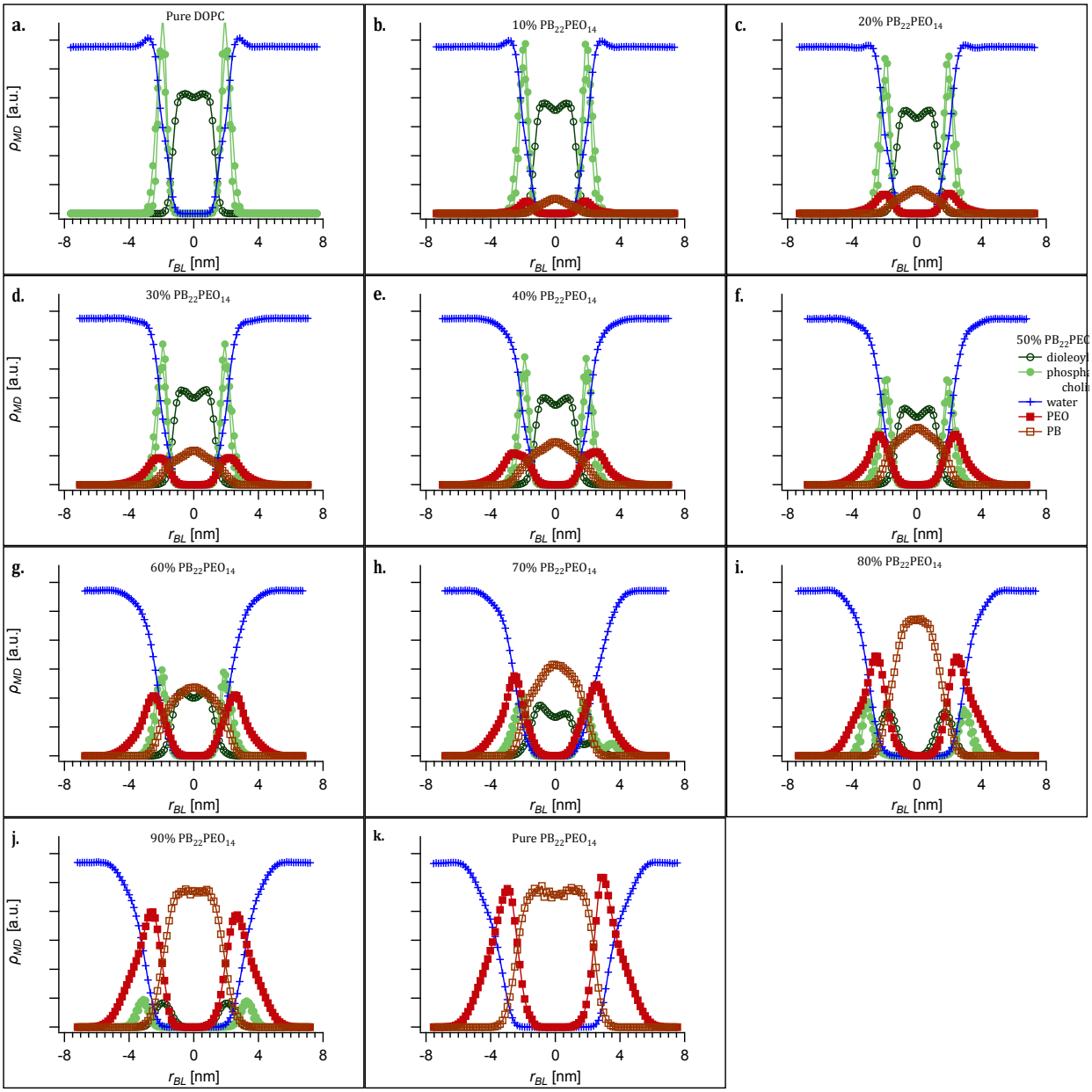

Figure S 14 contains the normalized electron density profiles for each molecular subspecies obtained from all of the CG MD simulation (10 μs) ; Each profile was obtained by averaging the dimension normal to the bilayer over the last 500 ns of the simulation.

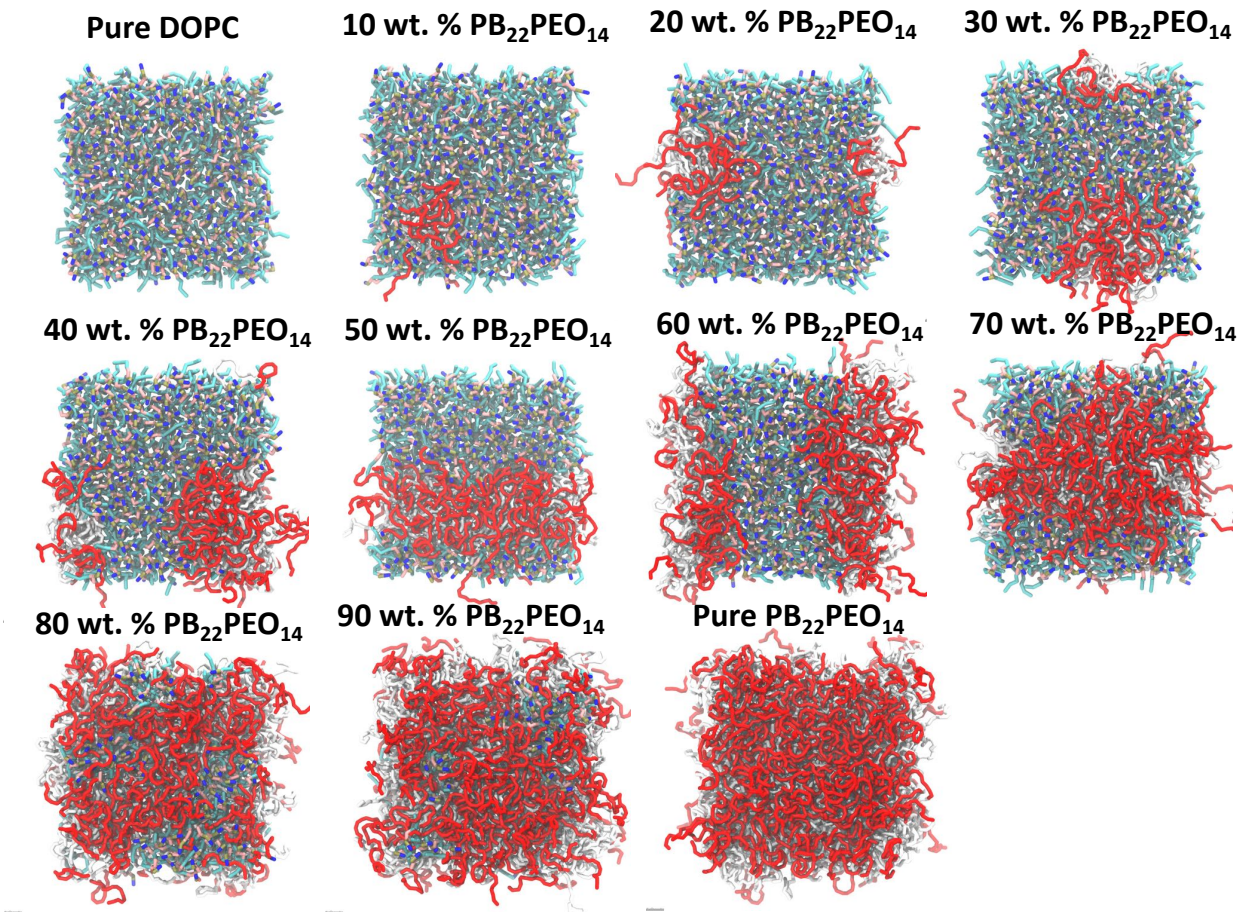

Figure S 15 contains the top views of the simulated hybrid bilayers for each molecular subspecies obtained from all of the CG MD simulation (10 μs) ; Each view is approximately 10 nm wide, and shows the spatial distribution of the PEO (red) and phosphate/choline (blue/brown) as a function of composition.

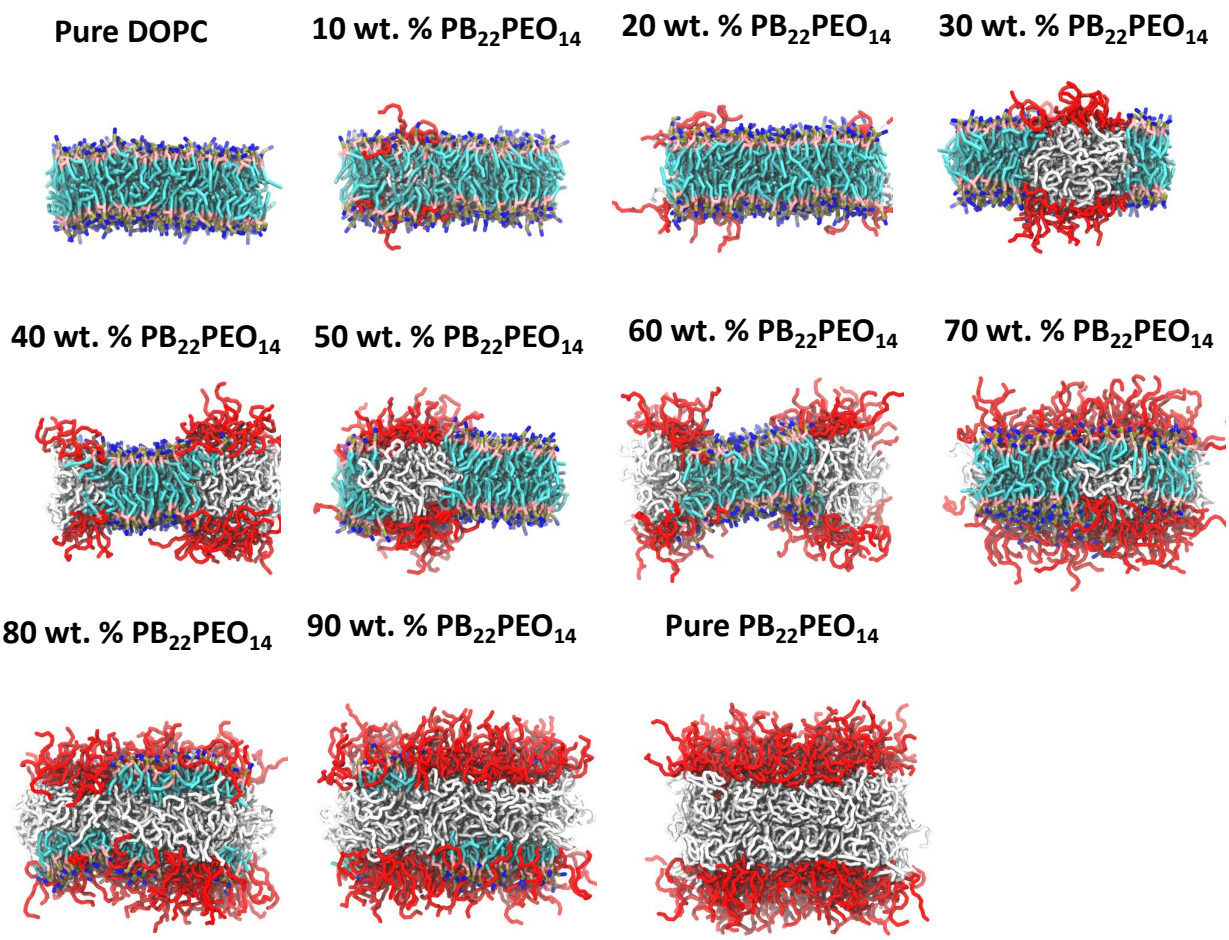

Figure S 16 contains the side views of the simulated hybrid bilayers for each molecular subspecies obtained from all of the CG MD simulation (10 μs) ; Each view is approximately 10 nm wide, and shows the spatial distribution of the PEO (red) and phosphate/choline (blue/brown) as a function of composition.

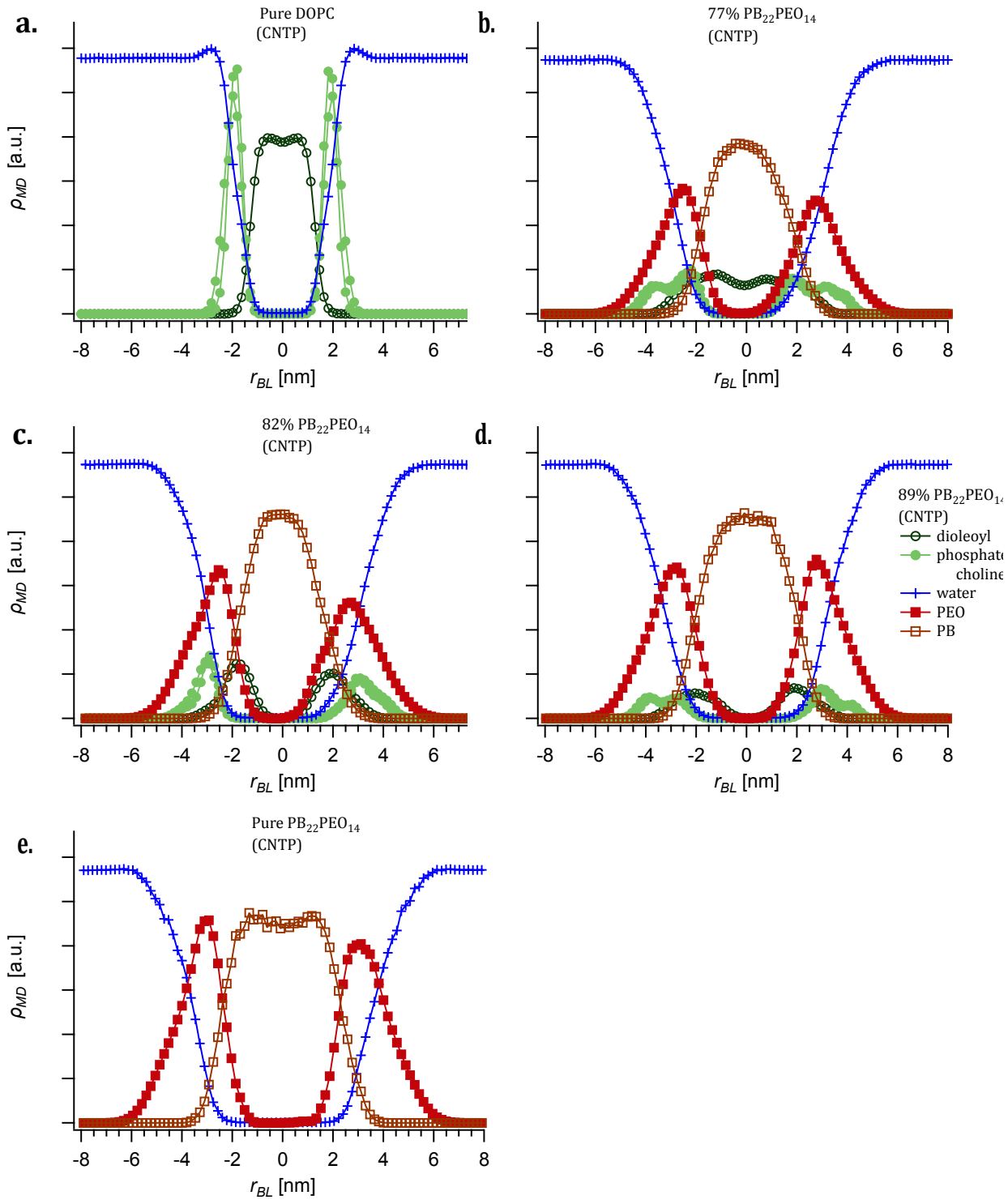

Figure S 17 contains the normalized electron density profiles for each molecular subspecies obtained from all of the CG MD simulation with one CNTP (10 μs) ; Each profile was obtained by averaging the dimension normal to the bilayer over the last 500 ns of the simulation.

S.2.B With CNTP

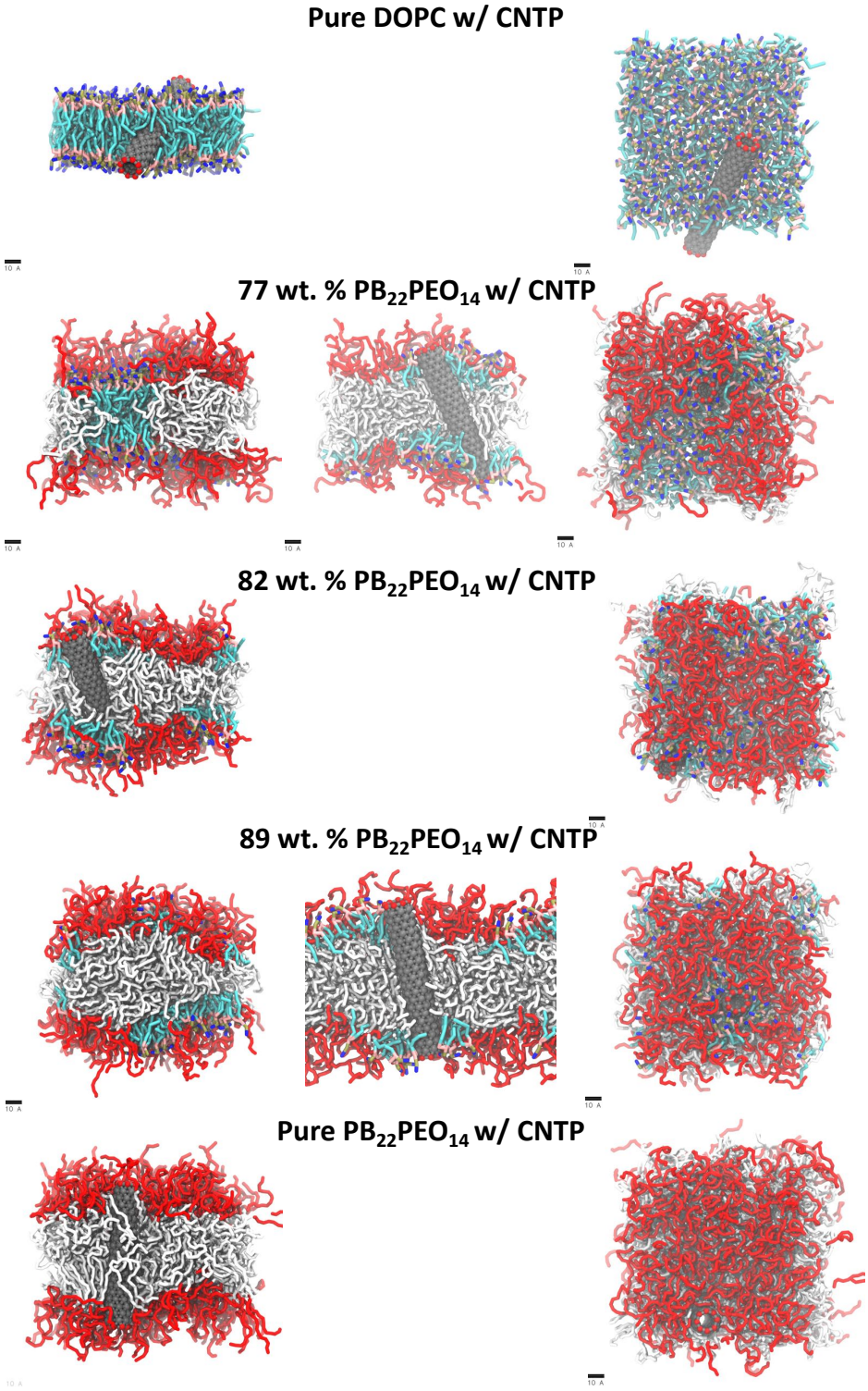

Figure S 18 contains the side and top views of the simulated hybrid bilayers for each molecular subspecies obtained from all of the CG MD simulation with CNTP (10 µs) ; Each view is approximately 10 nm wide, and shows the spatial distribution of the PEO (red) and phosphate/choline (blue/brown) as a function of composition.

S.2.C Simulation Time

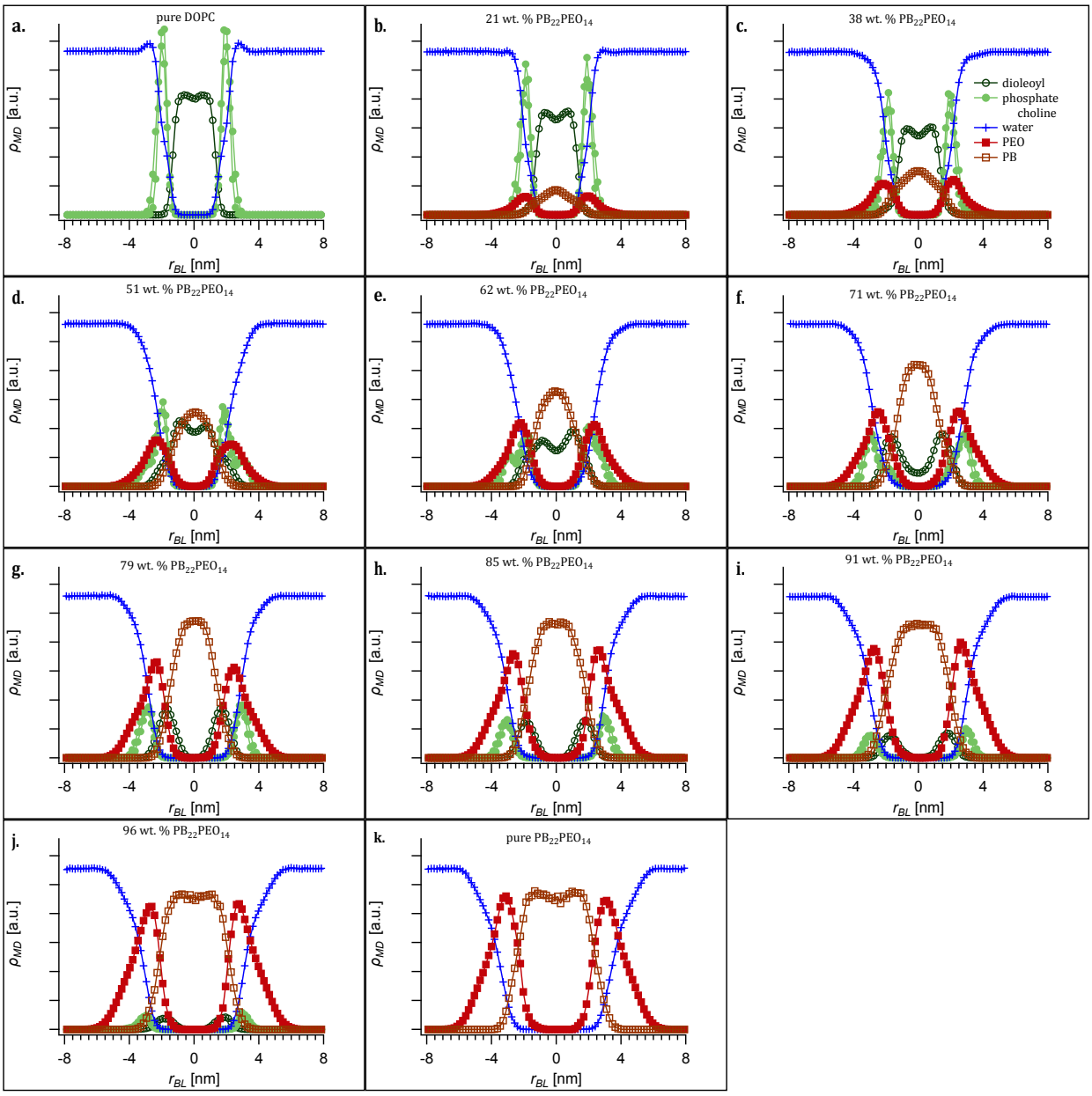

Figure S 19 contains the normalized electron density profiles for each molecular subspecies obtained from all of the CG MD simulation (1 μs) ; Each profile was obtained by averaging the dimension normal to the bilayer over the last 500 ns of the simulation.

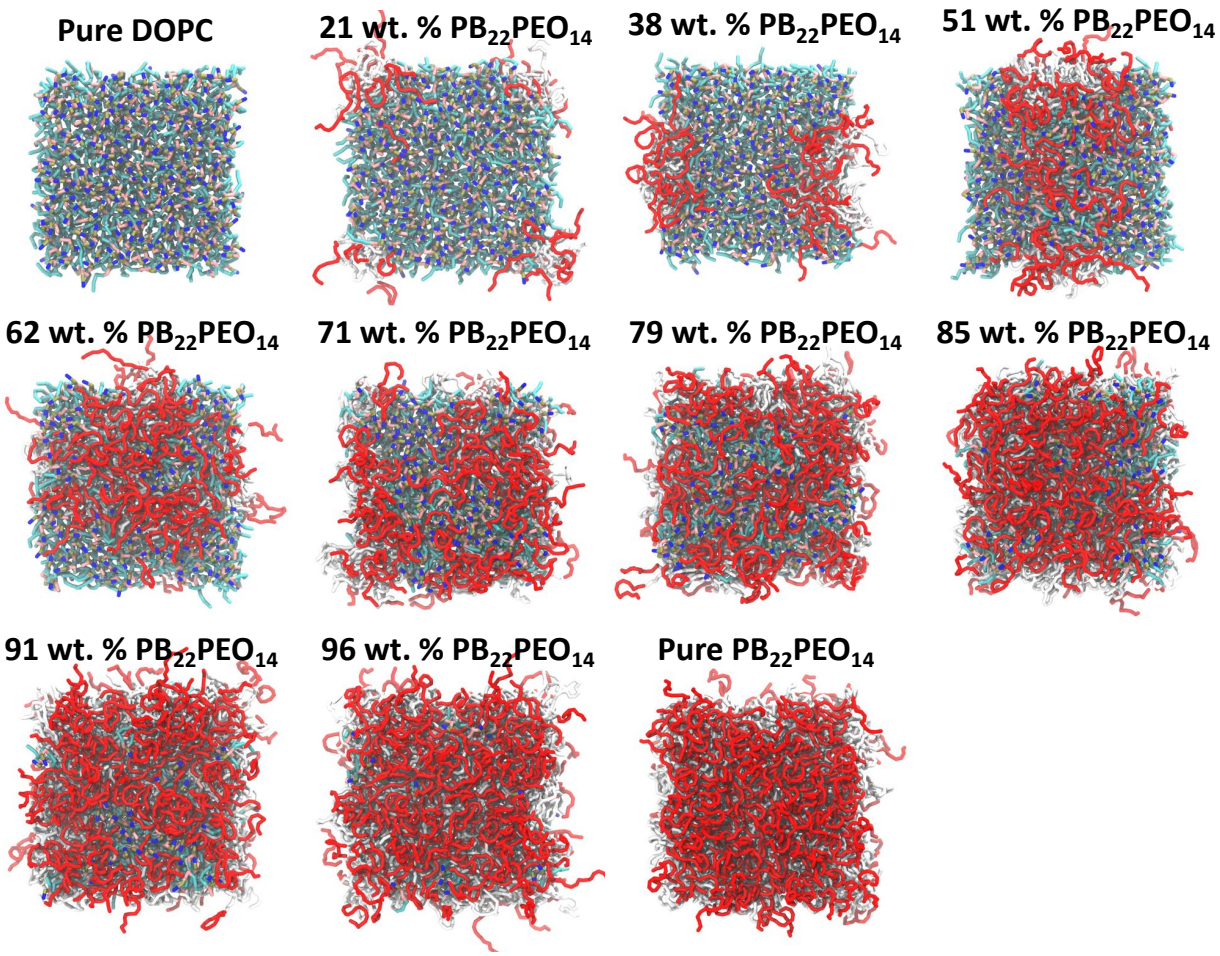

Figure S 20 contains the top views showing the spatial distribution of PB (white), PEO (red) and DO (cyan) PC (blue and brown) as a function of wt. % of $PB_{22}PEO_{14}$ obtained from CG MD simulation (1 μs)

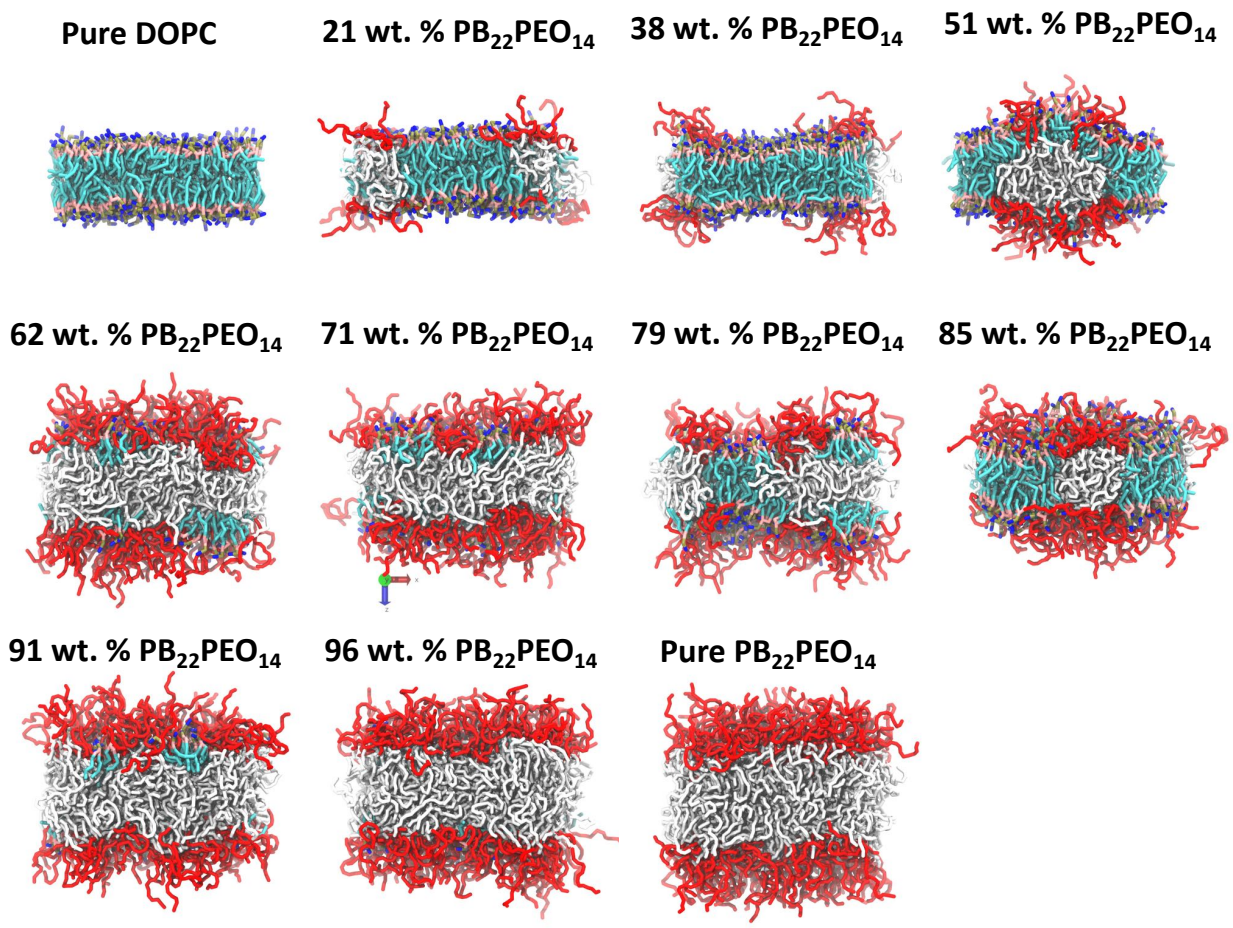

Figure S 21 is a plot comparing the estimated bilayer thickness obtained by SAXS from the PB-PEO/DOPC hybrid vesicles (black circles) and the PB-PEO/DOPC/CNTP vesicles (black diamonds) with the estimated thickness obtained from the coarse grain simulations that were run for 10 μs (blue shaded area). The nonlinear evolution of distance between opposing dioleoyl and PB groups, estimated from the FWHM, are shown as red squares and red open circles respectively.

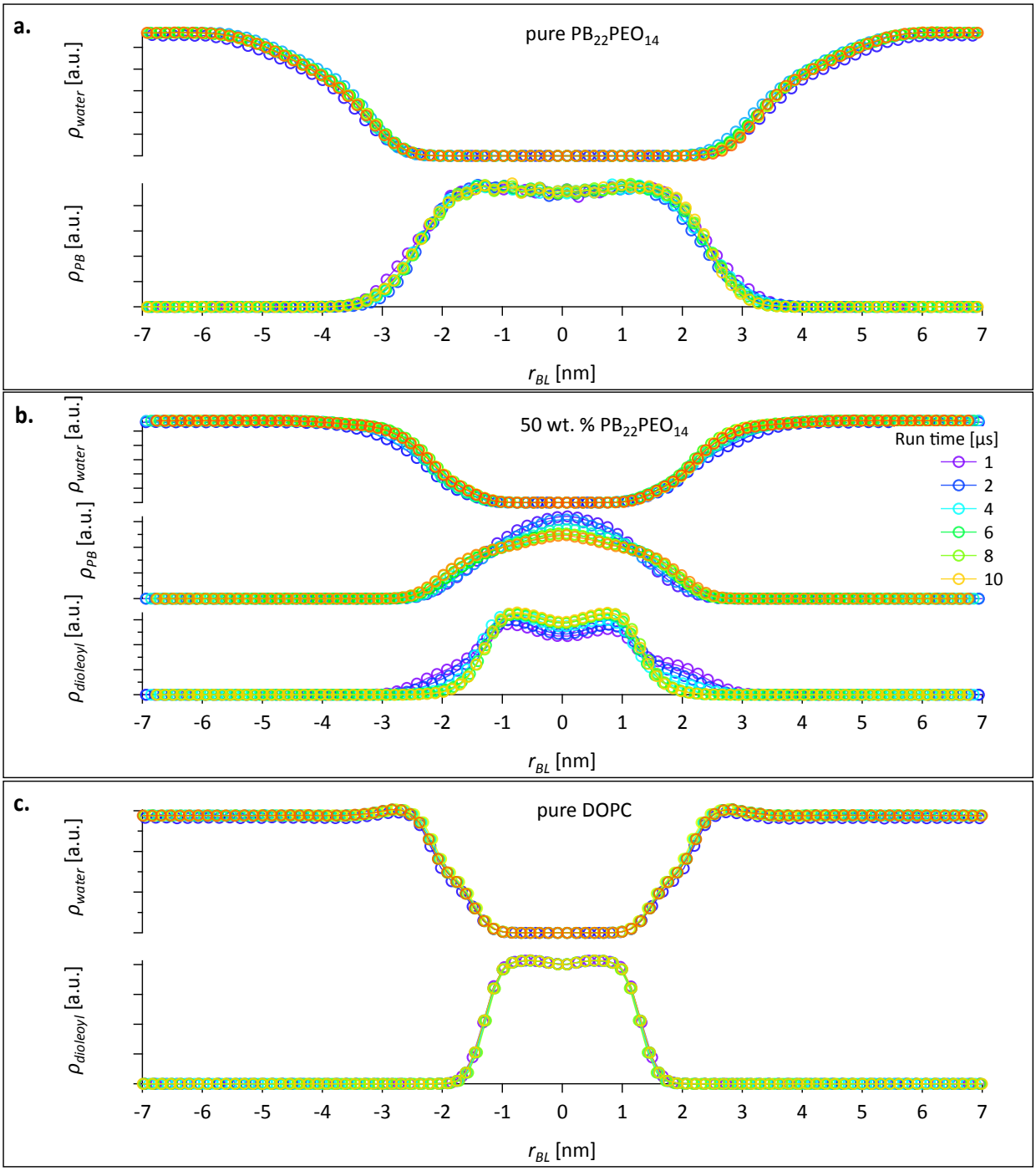

Figure S 22 three plots containing the normalized electron density profiles of different molecular species and sub groups as a function of simulation time shown in legend of Figure 16 b. Figure S 16 a contains the profiles of water (top plot) and PB (bottom plot) for the simulation of pure $PB_{22}PEO_{14}$. Figure 16 b contains profiles from water (top), PB (middle) and dioleoyl (bottom) from the 50 wt. % hybrid vesicle. Figure 16 c contains profiles from water (top) and dioleoyl (bottom) from pure DOPC.

S.3 Dioleoyl Distribution (10 µs and 1 µs) with Radial Electron Density Profiles Obtained from Simulated Annealing

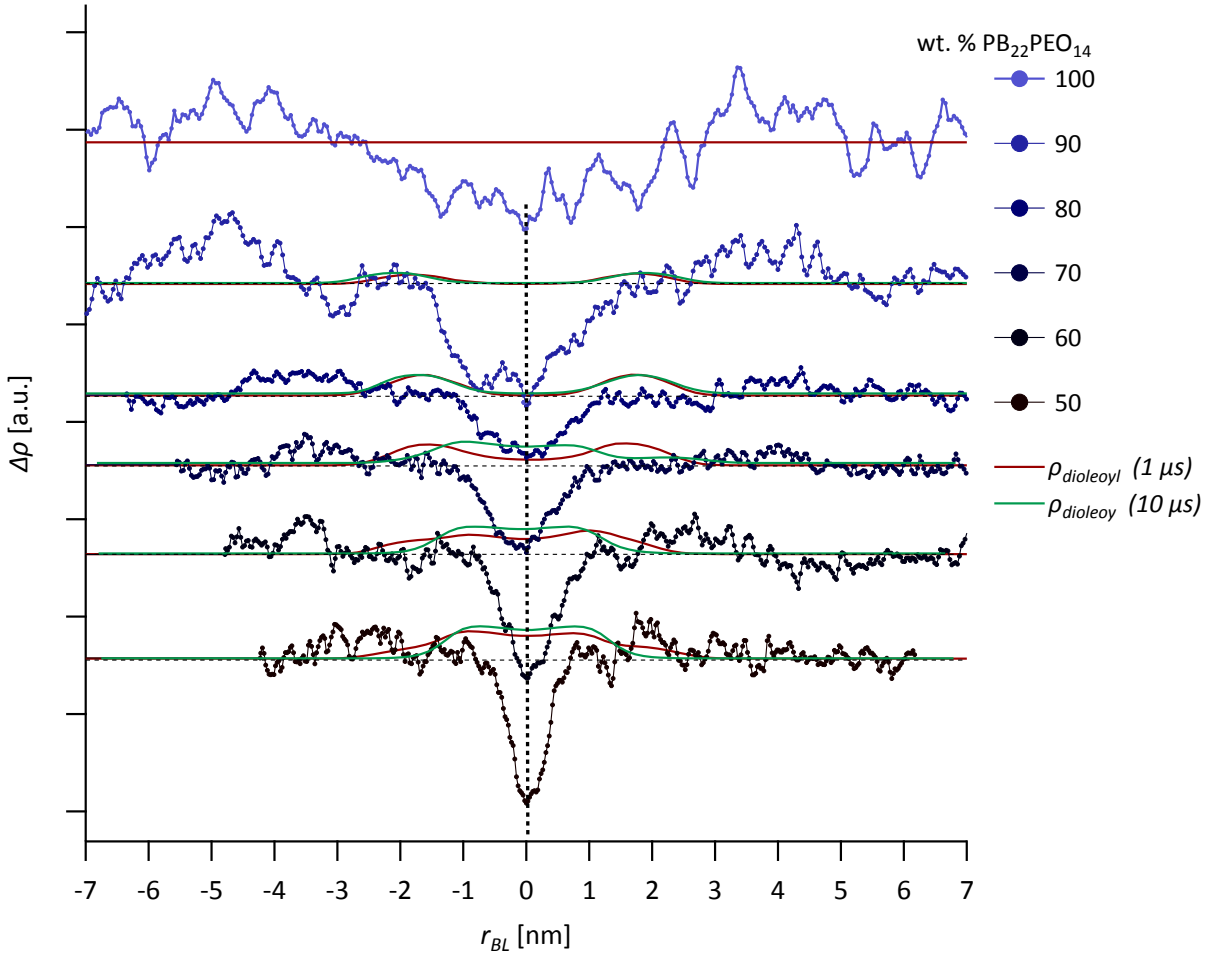

Figure S 23 is a plot comparing the radial bilayer contrast functions, Δρ(r_{BL}), obtained by simulated annealing of the SAXS data collected from the PB-PEO/DOPC hybrid vesicles. Starting from ~ 50 % $PB_{22}PEO_{14}$, the position of the broad dioleoyl peaks obtained from MD after both 1 µs (red) and 10 µs (green) can also be observed from the SAXS analysis at the same locations within the bilayer.

S.3 Cryo-TEM

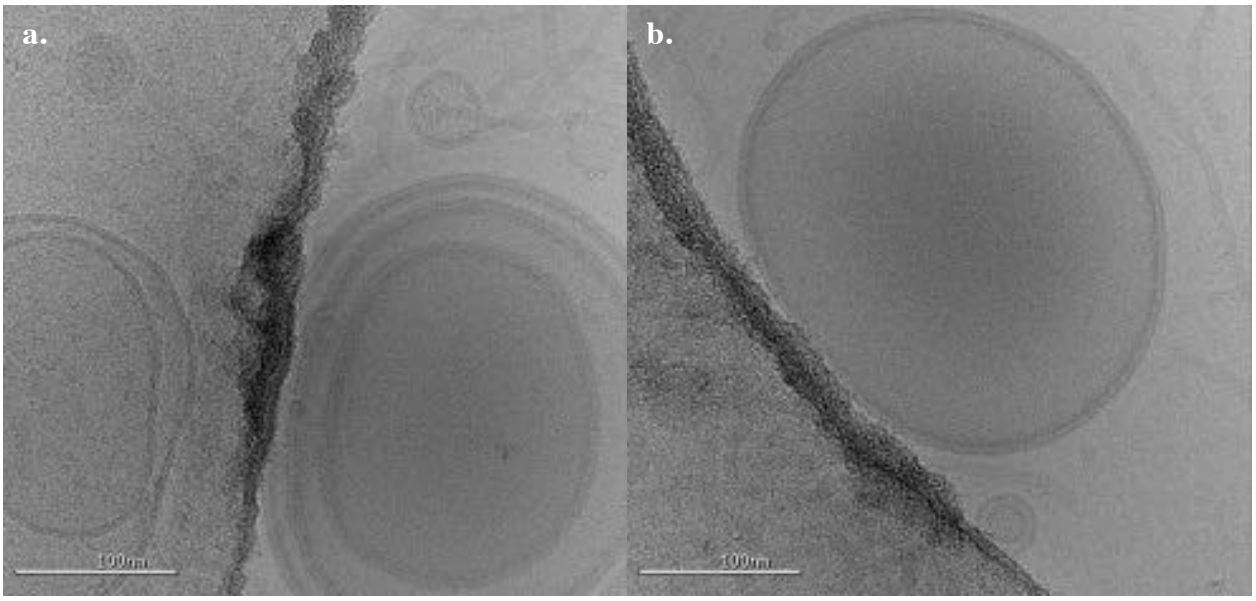

Figure S 24 multi-lamellar (a) and uni-lamellar (b) polymerosomes (pure $PB_{22}PEO_{14}$) observed by cryo-TEM

References

1. A. Guinier and G. Fournet, *Small-angle scattering of X-rays*, Wiley, New York,, 1955.
2. N. Kucerka, M. P. Nieh and J. Katsaras, *Langmuir*, 2009, **25**, 13522-13527.
3. J. Ilavsky, *J. Appl. Crystallogr.*, 2012, **45**, 324 – 328.